

DOI: 10.12158/j.2096-3203.2022.06.016

中低压电力电缆金属屏蔽接续状态带电测试技术

卞蓓蕾¹, 曹京荣², 刘鹏³

(1. 国网浙江省电力有限公司, 浙江 杭州 310007;

2. 国网江苏省电力有限公司电力科学研究院, 江苏 南京 211103;

3. 国网浙江省电力有限公司宁波供电公司, 浙江 宁波 315000)

摘要: 现有中低压电力电缆线路金属屏蔽连接不良时需要线路停役, 测试周期长且效率低, 针对该问题, 提出电缆金属屏蔽接地引线带电测试金属屏蔽电阻的方法。利用异频耦合测试电缆金属屏蔽感应电压和电流, 运用电磁感应及欧姆定律构建方程计算电缆金属屏蔽回路或支路电阻, 并通过电阻大小判断金属屏蔽连接状态。经实验室模拟测试发现, 在不改变原有接地状态时, 测试所得电缆金属屏蔽电阻参数与实际一致。单回路电缆线路受地网影响无法检测判别 $10\ \Omega$ 电阻以下的电缆金属屏蔽连接状态, 而双回路及以上电缆线路检测不易受地网影响, 可通过回路电阻、支路电阻与理论值比较, 或支路电阻相互比较判断电缆金属屏蔽的连接状态。检测技术经工程应用表明, 采用异频法带电检测金属屏蔽电阻, 进而判断中低压电缆金属屏蔽连接状态的方法具有可行性。

关键词: 中低压电力电缆; 金属屏蔽; 回路电阻; 带电测试; 异频耦合; 连接状态

中图分类号: TM724

文献标志码: A

文章编号: 2096-3203(2022)06-0134-06

0 引言

中低压电力电缆作为电网应用端的重要电气设备, 在城区配电网、变电站输电走廊等处应用广泛, 其安全水平关系电网运行的可靠性^[1-6]。中低压电力电缆采用品字型三芯统包结构, 使电缆三相电缆芯电流磁场相互抵消, 降低了钢带铠装电磁感应效应, 因此中低压电力电缆接地系统安装时广泛采用线路两端直接接地的方式^[7-9]。

受可运输成盘电缆长度影响, 一般长距离电缆线路需要加装接头, 并对电缆金属屏蔽等进行恢复和密封处理。由于电缆通道多位于地下, 空气潮湿且运行环境复杂, 当出现电缆或接头外护层密封不良问题时, 易造成电缆接头受潮或进水, 引起内部金属屏蔽锈蚀, 导致金属屏蔽连接不良或接地失效, 给电缆安全运行带来隐患^[10-15]。

传统电缆带电状态下的测试多采用红外测温或局放检测方法^[16-19]。由于电缆金属屏蔽连接缺陷多发于接头内部, 采用传统带电测试手段难以发现缺陷。传统停役状态下的测试一般采用直流回路电阻测试法, 该方法需要拆除接地引线, 改变原有接地方式且测试周期长, 不利于现场大范围普测^[20-21]。为此, 文中提出中低压电力电缆金属屏蔽连接状态带电测试方法, 用于解决中低压电力电缆

线路金属屏蔽接续状态带电测试的难题, 提高现场测试效率及缺陷发现率, 指导运维人员及时消缺。

1 电缆金属屏蔽传统测试方法

中低压电力电缆金属屏蔽层等效电路阻抗主要包含电阻、电感参数, 而电阻参数可直观反映电缆金属屏蔽连接状态, 因此传统检测方法主要采用直流回路电阻法。即在线路停役状态通过注入直流、检测电压参数, 获取电缆金属屏蔽回路电阻参数。直流回路电阻法需要将电缆金属屏蔽一侧的接地端断开, 注入直流电流测试直流电阻参数。

双回路电缆线路金属屏蔽直流回路电阻法原理为: $R_1 + R_2 = U_0 / I_0$ 。其中, R_1, R_2 分别为第 1 条、第 2 条支路电缆金属屏蔽电阻; I_0 为注入直流电流; U_0 为直流响应电压。三回路及以上电缆线路金属屏蔽直流回路电阻法原理为: $R_{ij} = U_{ij} / I_{ij} = R_i + R_j$ 。其中, $i \neq j$, i 和 j 为电缆金属屏蔽支路序号, 均为正整数; I_{ij} 为注入直流电流; U_{ij} 为注入直流电流对应的直流响应电压; R_{ij} 为支路 ij 电缆金属屏蔽的电阻。

中低压电力电缆金属屏蔽传统带电测试方法具有测试干扰小、接地处置灵活等优点, 但是需要线路停役并拆除接地引线, 测试周期长, 不利于大范围普测, 为此文中提出一种电缆金属屏蔽接续状态带电测试方法。

2 电缆金属屏蔽异频法电阻测试方法

2.1 单回路及双回路测试方法

采用异频耦合注入电缆金属屏蔽感应信号, 测

收稿日期: 2022-07-10; 修回日期: 2022-11-08

基金项目: 国家电网有限公司科技项目“计及老化劣化及局放多状态的电缆在线监测研究与应用”(5700-202118195A-0-0-00)

试获取感应电压、电流参数,并运用电磁感应和欧姆定律,计算获取电缆金属屏蔽电阻。双回路或单回路电缆金属屏蔽电阻异频法测试原理为:

$$\begin{cases} Z_{\omega_1} = R + X_{\omega_1} \\ Z_{\omega_2} = R + X_{\omega_2} \end{cases} \quad (1)$$

式中: ω_1, ω_2 为互不相等的角频率; $Z_{\omega_1}, Z_{\omega_2}$ 分别为角频率 ω_1 和 ω_2 下的回路阻抗; R 为回路电阻; $X_{\omega_1}, X_{\omega_2}$ 分别为角频率 ω_1 和 ω_2 下的回路感抗。

该方法可获取电缆金属屏蔽回路电阻,无法进一步带电识别支路电阻状态。

2.2 三回路测试方法

当电缆线路为三回路时,可通过测试电缆金属屏蔽回路电阻,组建联合方程计算各支路电阻。即依次对每回电缆金属屏蔽支路耦合激励3种频率的感应电压,并测试获取三回路支路感应电流。设第 y 回电缆金属屏蔽支路耦合激励感应电压有效值为 $U_{y\omega_i}$ 时,测试第 x 回电缆金属屏蔽支路感应电流为 $I_{xy\omega_i}$ 。其中, ω_i 为测试采用的角频率, $i=1,2,3$; $x=1,2,3$; $y=1,2,3$ 。

令 $Z_{x\omega_i} = R_x + j\omega_i L_x = R_x + jN_{x\omega_i}$ 。其中, $Z_{x\omega_i}$ 为第 x 回支路在角频率 ω_i 下的阻抗; R_x 为第 x 回支路电阻; L_x 为第 x 回支路电感; $N_{x\omega_i}$ 为第 x 回支路在角频率 ω_i 下的感抗。则:

$$\frac{Z_{1\omega_1}^2}{Z_{2\omega_1}^2} = \frac{R_1^2 + (\omega_1 L_1)^2}{R_2^2 + (\omega_1 L_2)^2} = \left(\frac{I_{23\omega_1}}{I_{13\omega_1}} \right)^2 = K_1^2 \quad (2)$$

$$\frac{Z_{1\omega_2}^2}{Z_{2\omega_2}^2} = \frac{R_1^2 + (\omega_2 L_1)^2}{R_2^2 + (\omega_2 L_2)^2} = \left(\frac{I_{23\omega_2}}{I_{13\omega_2}} \right)^2 = K_2^2 \quad (3)$$

$$\frac{Z_{1\omega_3}^2}{Z_{2\omega_3}^2} = \frac{R_1^2 + (\omega_3 L_1)^2}{R_2^2 + (\omega_3 L_2)^2} = \left(\frac{I_{23\omega_3}}{I_{13\omega_3}} \right)^2 = K_3^2 \quad (4)$$

$$\frac{Z_{3\omega_1}^2}{Z_{2\omega_1}^2} = \frac{R_3^2 + (\omega_1 L_3)^2}{R_2^2 + (\omega_1 L_2)^2} = \left(\frac{I_{21\omega_1}}{I_{31\omega_1}} \right)^2 = K_4^2 \quad (5)$$

$$\frac{Z_{3\omega_2}^2}{Z_{2\omega_2}^2} = \frac{R_3^2 + (\omega_2 L_3)^2}{R_2^2 + (\omega_2 L_2)^2} = \left(\frac{I_{21\omega_2}}{I_{31\omega_2}} \right)^2 = K_5^2 \quad (6)$$

$$\frac{Z_{3\omega_3}^2}{Z_{2\omega_3}^2} = \frac{R_3^2 + (\omega_3 L_3)^2}{R_2^2 + (\omega_3 L_2)^2} = \left(\frac{I_{21\omega_3}}{I_{31\omega_3}} \right)^2 = K_6^2 \quad (7)$$

式中: K_1-K_6 为中间变量。则由式(2)一式(4)可得:

$$\frac{R_1^2}{R_2^2} = \frac{(\omega_2^2 K_1^2 - \omega_1^2 K_2^2) - \delta_1(\omega_3^2 K_2^2 - \omega_2^2 K_3^2)}{(\omega_2^2 - \omega_1^2) - \delta_1(\omega_3^2 + \omega_2^2)} \quad (8)$$

$$\frac{L_1^2}{L_2^2} = \frac{(\omega_1^2 K_1^2 - \omega_2^2 K_2^2) - \delta_2(\omega_3^2 K_3^2 - \omega_2^2 K_2^2)}{(\omega_1^2 - \omega_2^2) - \delta_2(\omega_3^2 - \omega_2^2)} \quad (9)$$

$$\text{式中: } \delta_1 = \frac{(K_1^2 - K_2^2) \omega_1^2}{(K_2^2 - K_3^2) \omega_3^2}; \delta_2 = \frac{(K_1^2 - K_2^2)}{(K_3^2 - K_2^2)}。$$

同理,由式(5)一式(7)可得:

$$\frac{R_3^2}{R_2^2} = \frac{(\omega_2^2 K_4^2 - \omega_1^2 K_5^2) - \delta_3(\omega_3^2 K_5^2 - \omega_2^2 K_6^2)}{(\omega_2^2 - \omega_1^2) - \delta_3(\omega_3^2 + \omega_2^2)} \quad (10)$$

$$\frac{L_3^2}{L_2^2} = \frac{(\omega_1^2 K_4^2 - \omega_2^2 K_5^2) - \delta_4(\omega_3^2 K_6^2 - \omega_2^2 K_5^2)}{(\omega_1^2 - \omega_2^2) - \delta_4(\omega_3^2 - \omega_2^2)} \quad (11)$$

$$\text{式中: } \delta_3 = \frac{(K_4^2 - K_5^2) \omega_1^2}{(K_5^2 - K_6^2) \omega_3^2}; \delta_4 = \frac{(K_4^2 - K_5^2)}{(K_6^2 - K_5^2)}。$$

令 $R_1/R_2 = X_1; R_3/R_2 = X_2; L_1/L_2 = Y_1; L_3/L_2 = Y_2; N_{2\omega_1}^2/R_2^2 = M_1; N_{2\omega_2}^2/R_2^2 = M_2$ 。其中, $X_1, X_2, Y_1, Y_2, M_1, M_2$ 为中间参量,则:

$$\frac{R_2^2 [(\alpha - \beta M_1)^2 + \eta^2 M_1]}{\theta^2 + \varepsilon^2 M_1} = \left(\frac{U_{1\omega_1}}{I_{1\omega_1}} \right)^2 = Z_{1(\omega_1)}^2 \quad (12)$$

$$\frac{R_2^2 [(\alpha - \beta M_2)^2 + \eta^2 M_2]}{\theta^2 + \varepsilon^2 M_2} = \left(\frac{U_{1\omega_2}}{I_{1\omega_2}} \right)^2 = Z_{1(\omega_2)}^2 \quad (13)$$

式中: $\alpha = X_1 + X_2 + X_1 X_2; \beta = Y_1 + Y_2 + Y_1 Y_2; \eta = X_1 + X_2 + Y_1 + Y_2 + X_1 Y_2 + X_2 Y_1; \theta = X_1 + X_2; \varepsilon = Y_1 + Y_2; Z_{1(\omega_1)}, Z_{1(\omega_2)}$ 分别为第2回支路某点断开后两侧在角频率 ω_1 和 ω_2 下的等效阻抗。

联立式(12)、式(13)可得:

$$\frac{R_2^2 [(\alpha - \beta M_1)^2 + \eta^2 M_1]}{\theta^2 + \varepsilon^2 M_1} \times \frac{\theta^2 + \varepsilon^2 M_2}{R_2^2 [(\alpha - \beta M_2)^2 + \eta^2 M_2]} = \frac{Z_{1(\omega_1)}^2}{Z_{1(\omega_2)}^2} = T \quad (14)$$

令 $P = M_2/M_1; a = \beta^2 \varepsilon^2 (P - P^2 T); b = \beta^2 \theta^2 (1 - P^2 \times T) + \varepsilon^2 (\eta^2 - 2\alpha\beta) P (1 - T); c = \varepsilon^2 \alpha^2 (P - T) + (\eta^2 - 2\alpha\beta) \times \theta^2 (1 - TP); d = \alpha^2 \theta^2 (1 - T)$ 。则化简式(14)可以得到:

$$M_1^3 + \frac{b}{a} M_1^2 + \frac{c}{a} M_1 + \frac{d}{a} = 0 \quad (15)$$

求解实数解 M_1 ,代入式(12)可得:

$$R_2 = \sqrt{\frac{Z_{1(\omega_1)}^2 (\theta^2 + \varepsilon^2 M_1)}{(\alpha - \beta M_1)^2 + (\eta^2 M_1)}} \quad (16)$$

利用 R_1, R_3 与 R_2 的关系计算获得 R_1 和 R_3 电阻值。通过 R_1-R_3 电阻与理论值的比较,或相互比较,当出现与理论值严重不符或两两支路电阻相差较大时,判断电缆金属屏蔽存在连接缺陷。

2.3 四回路及以上测试方法

四回路及以上电缆金属屏蔽电阻测试方法与

三回路测试方法一致,即任选2个支路作为独立支路,剩余支路合并为1个支路进行测试,并按照三回路电缆金属屏蔽异频法测试获取各支路电缆金属屏蔽电阻。例如针对编号为1—4的四回路电缆线路,将第3和第4支路合并作为1个支路后,与第1和第2支路按照三回路电缆金属屏蔽异频法测试,可获得第1和第2支路金属屏蔽电阻,同理第1和第2支路合并后与第3和第4支路按照三回路电缆金属屏蔽异频法测试,可获得第3和第4支路金属屏蔽电阻。

3 实验室模拟测试

3.1 单回路模拟测试

为模拟单回路电缆金属屏蔽接续不良缺陷,在电缆接地引线串接可调电阻模拟接触电阻变化。通过调节可调电阻,测试获取回路电阻参数,试验接线如图1所示。

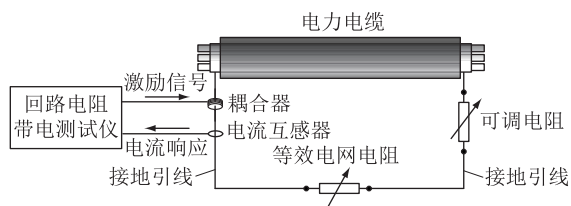


图1 单回路电缆模拟试验接线
Fig.1 Wiring of single-circuit cable simulation test

测试时不改变原有接地状态,现场测试回路含地网,因此测试结果受地网电阻的影响。依据 GB 50150—2016 规定,地网电阻一般不超过 10 Ω。对于回路电阻小于 10 Ω 的测试结果,因地网电阻未知且波动,现场无法判断单支路电缆金属屏蔽连接状态,但对远大于地网电阻的回路电阻测试结果,如回路电阻为无穷大时可判断为电缆金属屏蔽连接不良。

3.2 双回路模拟测试

模拟双回路电缆金属屏蔽电阻测试,如图2所示,在两回路电缆之间并联一可调电阻模拟等效地网电阻,测试分析地网电阻对电缆金属屏蔽回路电阻的影响。

测试时不改变原有接地状态,由于电缆金属屏蔽阻值水平远小于地网电阻,正常状态下地网电阻对双回路电缆金属屏蔽电阻测试影响较小,如图3所示。现场检测可通过与电缆金属屏蔽理论回路电阻值比较,判断是否存在缺陷。其缺点是当检测回路电阻异常时,无法判断是其中单回还是双回电缆金属屏蔽存在问题。

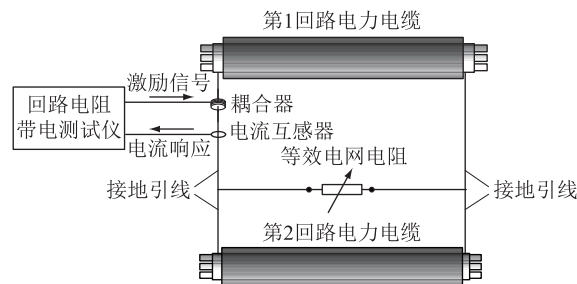


图2 双回路电缆模拟试验接线
Fig.2 Wiring of double-circuit cable simulation test

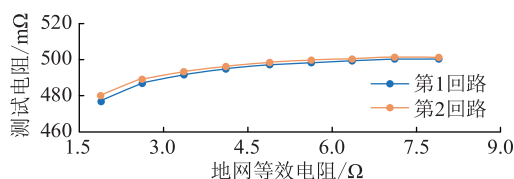


图3 地网电阻对双回路电缆金属屏蔽电阻影响
Fig.3 Influence of ground grid resistance on metal shielding resistance of double-circuit cable

3.3 三回路模拟测试

模拟三回路电缆金属屏蔽电阻测试,如图4所示。三回路电缆线路金属屏蔽首末端短接,并行串接一可调电阻模拟地网电阻。在第1回路电缆金属屏蔽串接可调电阻模拟金属屏蔽连接不良缺陷。

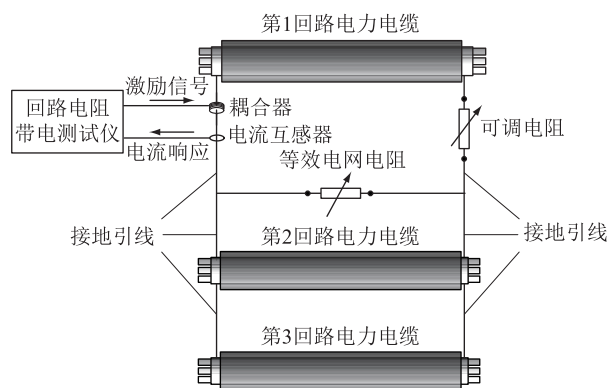


图4 三回路电缆模拟试验接线
Fig.4 Wiring of three-circuit cable simulation test

测试时不改变原有接地状态,利用2.2节提出的测试方法,测试获取电缆各支路金属屏蔽电阻参数,测试结果与实际一致,且发现正常状态下地网电阻变化对三回路电缆金属屏蔽各支路电阻测试结果影响较小,如图5所示。

针对三回路及以上电缆金属屏蔽检测数据,除与理论值比较外,也可通过支路电阻相互比较来判断电缆金属屏蔽连接状态,当出现与理论值严重不符或两两支路电阻相差较大时,判断电缆金属屏蔽存在连接缺陷。

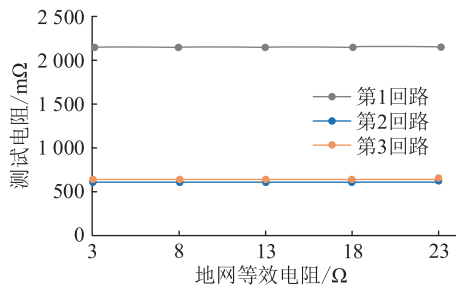


图5 地网电阻对三回路电缆金属屏蔽电阻影响

Fig.5 Influence of ground grid resistance on metal shielding resistance of three-circuit cable

4 工程案例应用

两变电站之间并行敷设编号1—3的三回路10 kV中压电缆,且电缆进出线首末端电缆金属屏蔽均接地。带电状态下对三回路电缆接地引线开展回路电阻测试,第1回电缆金属屏蔽耦合激励感应电压,测试第1—3回电缆金属屏蔽感应电流见表1。

表1 第1回电缆回路激励感应后各支路测试数据

Table 1 Test data of each branch after excitation induction of the first cable loop

序列	$\omega_i/(\text{rad}\cdot\text{s}^{-1})$	U_{1_oi}/V	I_{11_oi}/A	I_{21_oi}/A	I_{31_oi}/A
$i=1$	439.82	0.900	1.611	0.204	1.449
$i=2$	502.65	1.100	1.845	0.250	1.654
$i=3$	628.32	1.300	1.922	0.296	1.708

第2回电缆金属屏蔽耦合激励感应电压,测试第1—3回电缆金属屏蔽感应电流见表2。

表2 第2回电缆回路激励感应后各支路测试数据

Table 2 Test data of each branch after excitation induction of the second cable loop

序列	$\omega_i/(\text{rad}\cdot\text{s}^{-1})$	U_{2_oi}/V	I_{12_oi}/A	I_{22_oi}/A	I_{32_oi}/A
$i=1$	439.82	0.423	0.204	0.423	0.219
$i=2$	502.65	0.609	0.295	0.609	0.314
$i=3$	628.32	0.511	0.250	0.511	0.261

第3回电缆金属屏蔽耦合激励感应电压,测试第1—3回电缆金属屏蔽感应电流见表3。

表3 第3回电缆回路激励感应后各支路测试数据

Table 3 Test data of each branch after excitation induction of the third cable loop

序列	$\omega_i/(\text{rad}\cdot\text{s}^{-1})$	U_{3_oi}/V	I_{13_oi}/A	I_{23_oi}/A	I_{33_oi}/A
$i=1$	439.82	0.900	1.449	0.219	1.633
$i=2$	502.65	1.200	1.804	0.290	2.041
$i=3$	628.32	1.100	1.445	0.261	1.648

将表1—表3数据代入式(2)—式(16)计算可得: $R_1=0.231\ \Omega$; $R_2=2.001\ \Omega$, $R_3=0.198\ \Omega$ 。对比分析第2回电缆金属屏蔽电阻约为第1、3回路电阻的8~10倍,且远超理论电阻水平,判断存在金属屏蔽连接不良缺陷。经现场停役检查发现第2回电缆线路接头铜编织线与电缆金属屏蔽及钢带接触不良,验证了文中检测方法的可行性。

5 结论

(1) 采用异频法可检测中低压电力电缆金属屏蔽回路电阻,并通过回路电阻评判电缆金属屏蔽连接状态,检测不需要电缆线路停役且不改变原有接地状态。

(2) 单回路电缆线路可利用地网构成回路检测电缆金属屏蔽连接状态,因地网电阻未知且波动,检测无法判断10 Ω 电阻以下的电缆金属屏蔽连接状态。

(3) 双回路及以上电缆金属屏蔽回路电阻检测不易受地网电阻波动影响,可通过回路或支路电阻大小、支路电阻互比数据判断电缆金属屏蔽连接状态。

参考文献:

- [1] 史传卿. 电力电缆[M]. 北京:中国电力出版社,2006. SHI Chuanqing. Power cable[M]. Beijing: China Electric Power Press,2006.
- [2] 罗俊华,邱毓昌,杨黎明. 10 kV及以上电力电缆运行故障统计分析[J]. 高电压技术,2003,29(6):14-16. LUO Junhua, QIU Yuchang, YANG Liming. Operation fault analysis of CLPE power cable above 10 kV[J]. High Voltage Engineering,2003,29(6):14-16.
- [3] 唐志平,邹一琴. 供配电技术[M].4版. 北京:电子工业出版社,2019. TANG Zhiping, ZOU Yiqin. Power supply and distribution technology[M]. 4th ed. Beijing: Publishing House of Electronics Industry,2019.
- [4] DESSOUKY S, ZEIN A, ABD EL-AAL R A, et al. Analysis of the electric field distribution within MV cable joint in the presence of defects in cable insulation[J]. International Journal of Applied Energy Systems,2019,1(1):35-44.
- [5] 中华人民共和国住房和城乡建设部. 电气装置安装工程 电气设备交接试验标准:GB 50150—2016[S]. 北京:中国计划出版社,2016. Ministry of Housing and Urban-Rural Development of the People's Republic of China. Electric equipment installation engineering-standard for hand-over test of electric equipment: GB 50150-2016[S]. Beijing: China Planning Press,2016.
- [6] 聂永杰,赵现平,李盛涛. XLPE电缆状态监测与绝缘诊断研究进展[J]. 高电压技术,2020,46(4):1361-1371. NIE Yongjie, ZHAO Xianping, LI Shengtao. Research progress

- in condition monitoring and insulation diagnosis of XLPE cable [J]. High Voltage Engineering, 2020, 46(4): 1361-1371.
- [7] 中华人民共和国住房和城乡建设部. 电力工程电缆设计标准: GB 50217—2018[S]. 北京: 中国计划出版社, 2018. Ministry of Housing and Urban-Rural Development of the People's Republic of China. Standard for design of cables of electric power engineering: GB 50217-2018 [S]. Beijing: China Planning Press, 2018.
- [8] 朱启林, 李仁义, 徐丙垠. 电力电缆故障测试方法与案例分析[M]. 北京: 机械工业出版社, 2008. ZHU Qilin, LI Renyi, XU Bingyin. Test method and case analysis of power cable fault [M]. Beijing: China Machine Press, 2008.
- [9] 彭楠, 张鹏, 梁睿. 基于暂态特征模量分析的配网三芯铠装电缆故障感知与测距[J]. 中国电机工程学报, 2021, 41(16): 5767-5779. PENG Nan, ZHANG Peng, LIANG Rui. Fault sensing and location of the three-core armored cables in distribution network based on the analysis of the fault-featured transient moduli [J]. Proceedings of the CSEE, 2021, 41(16): 5767-5779.
- [10] 杨帆, 曾蕊, 阮羚, 等. 中压交联电缆接头复合界面受潮缺陷的诊断方法研究[J]. 高压电器, 2014, 50(5): 1-5. YANG Fan, ZENG Chun, RUAN Ling, et al. Study on diagnostic method of compound boundary in medium voltage cross-linked cable joints moistened [J]. High Voltage Apparatus, 2014, 50(5): 1-5.
- [11] 方春华, 叶小源, 杨司齐, 等. 水分对 XLPE 电缆中间接头电场和击穿电压的影响[J]. 华北电力大学学报(自然科学版), 2021, 48(2): 64-72. FANG Chunhua, YE Xiaoyuan, YANG Siqi, et al. Effect of moisture on electric field and breakdown voltage at XLPE cable intermediate joint [J]. Journal of North China Electric Power University (Natural Science Edition), 2021, 48(2): 64-72.
- [12] 李巍巍, 朱轲, 吴驰, 等. 不同温度下受潮电缆终端头的绝缘状态研究[J]. 环境技术, 2016, 34(4): 6-10, 23. LI Weiwei, ZHU Ke, WU Chi, et al. Research on insulation condition of damp cable joint under different temperatures [J]. Environmental Technology, 2016, 34(4): 6-10, 23.
- [13] 袁野, 陈剑, 贾志东, 等. 10 kV XLPE 电缆受潮绝缘特性研究[J]. 电网技术, 2014, 38(10): 2875-2880. YUAN Ye, CHEN Jian, JIA Zhidong, et al. Study about insulating properties of 10 kV XLPE damp cable [J]. Power System Technology, 2014, 38(10): 2875-2880.
- [14] 张丹丹, 苏小婷, 景晓东, 等. 基于阻抗谱的同轴电缆故障及中间接头定位实验研究[J]. 高压电器, 2021, 57(7): 92-97, 104. ZHANG Dandan, SU Xiaoting, JING Xiaodong, et al. Experimental study on coaxial cable faults and intermediate joints location based on impedance spectrum [J]. High Voltage Apparatus, 2021, 57(7): 92-97, 104.
- [15] 李蓉, 周凯, 饶显杰, 等. 基于输入阻抗谱的电缆故障类型识别及定位[J]. 高电压技术, 2021, 47(9): 3236-3245. LI Rong, ZHOU Kai, RAO Xianjie, et al. Identification and location of cable faults based on input impedance spectrum [J]. High Voltage Engineering, 2021, 47(9): 3236-3245.
- [16] 张若兵, 陈子豪, 杜钢. 适用于振荡波电缆局放测试的 π 型检测阻抗设计[J]. 高电压技术, 2019, 45(5): 1503-1509. ZHANG Ruobing, CHEN Zihao, DU Gang. Design of π -type detection impedance for oscillatory wave cable partial discharge test [J]. High Voltage Engineering, 2019, 45(5): 1503-1509.
- [17] 黄韬, 郝艳捧, 肖佳朋, 等. 10 kV XLPE 电缆终端典型安装缺陷的工频局部放电特征对比研究[J]. 电网技术, 2022, 46(6): 2420-2428. HUANG Tao, HAO Yanpeng, XIAO Jiapeng, et al. Comparative study on partial discharge characteristics of typical installation defects in 10 kV XLPE cable terminals under power frequency [J]. Power System Technology, 2022, 46(6): 2420-2428.
- [18] 傅尧, 周凯, 朱光亚, 等. 一种基于改进的 WGAN 模型的电缆终端局部放电识别准确率提升方法[J]. 电网技术, 2022, 46(5): 2000-2008. FU Yao, ZHOU Kai, ZHU Guangya, et al. Accuracy improvement of cable termination partial discharging recognition based on improved WGAN algorithm [J]. Power System Technology, 2022, 46(5): 2000-2008.
- [19] 周达, 张昕, 邹云峰, 等. 基于 T-F 聚类和 PRPD 图谱分析的配网电缆局部放电类型识别研究[J]. 电气工程学报, 2022, 17(2): 235-242. ZHOU Da, ZHANG Xin, ZOU Yunfeng, et al. Study on partial discharge pattern recognition for distribution cable based on T-F clustering and PRPD spectrum analysis [J]. Journal of Electrical Engineering, 2022, 17(2): 235-242.
- [20] 邵锦滔. 配网电缆故障定位技术的分析与应用[D]. 广州: 华南理工大学, 2019. SHAO Jintao. Application practice and analysis research of cable fault location method [D]. Guangzhou: South China University of Technology, 2019.
- [21] 岳晋. 电力电缆故障查找方法与测距分析研究[D]. 天津: 天津大学, 2013. YUE Jin. Research on power fault finding method and ranging analysis [D]. Tianjin: Tianjin University, 2013.

作者简介:



卞蓓蕾

卞蓓蕾(1971),女,硕士,高级工程师,从事电力系统相关工作(E-mail:bianbeilei@126.com);

曹京荣(1987),男,硕士,高级工程师,从事电力电缆运维、质量检测及可靠性评价工作;

刘鹏(1984),男,硕士,高级工程师,从事电力系统设备管理、电力信息通信相关工作。

Live test technology for metal shielding of medium and low voltage power cables in continuous state

BIAN Beilei¹, CAO Jingying², LIU Peng³

(1. State Grid Zhejiang Electric Power Co., Ltd., Hangzhou 310007, China;

2. State Grid Jiangsu Electric Power Co., Ltd. Research Institute, Nanjing 211103, China;

3. State Grid Ningbo Power Supply Company of Zhejiang Electric Power Co., Ltd., Ningbo 315000, China)

Abstract: The defects of poor metal shielding connection of medium and low voltage cable lines are tested for a long time, which requires the lines are out of service. A method to measure the resistance of cable metal shield circuit by using different frequency coupling is presented. Combined with electromagnetic induction law and Ohm's law, the circuit resistance or branch resistance is calculated by constructed simultaneous equations, which is used for judging the connection state of metal shielding. Through laboratory simulation test, it is found that the test cable metal shielding resistance parameters are consistent with the actual values when the original grounding state is not changed. The connection state of cable metal shielding with resistance below 10Ω can not be detected and judged for single-circuit cable lines. While double-circuit and above cable lines are not easy to be affected by the grounding grid, and the connection state of cable metal shielding can be judged by comparing the circuit resistance and branch resistance with theoretical value, or by comparing the branch resistance with each other. The detection technology is verified by the engineering application, which is effective and feasible to judge the metal shielding connection state for medium and low voltage cables.

Keywords: medium and low voltage cables; metal shielding; loop resistance; live test; different frequency coupling; connection status

(编辑 吴楠)

(上接第 81 页)

Coordinate control strategy of VSC-MTDC based on model predictive control

MA Wenzhong¹, GUAN Zengjia¹, ZHANG Kuitong², ZHANG Yan², YAO Minrui¹, LI Mushu¹

(1. College of New Energy, China University of Petroleum (East China), Qingdao 266580, China;

2. Shandong Energy Group Co., Ltd., Jinan 250014, China)

Abstract: The voltage-source converter based multi-terminal direct current (VSC-MTDC) transmission system is mainly applied in grid-connection and long-distance transmission of new energy power generation. New energy power generation has volatility and uncertainty. When using traditional droop control strategy, VSC will be overloaded due to uneven power distribution, protection malfunction will be caused by excessive DC voltage deviation, and oscillation will occur due to communication delay. Therefore, a coordinated control strategy based on model predictive control (MPC) is proposed in this paper. The strategy optimizes parameters according to system state and sends VSC power reference, eliminating the influence of droop coefficient, line resistance and system topology on power allocation. The robustness of MPC also improves the stability of the system in the case of communication delay. The four terminal VSC-MTDC model is built in Simulink, and different operating conditions are set for time-domain simulation. The simulation results show that the control strategy can quickly adjust the converter station power and control the DC voltage when the system is disturbed, and ensure the system stability when the communication delay occurs, so as to improve the adaptability of the power system to the fluctuation and uncertainty of new energy generation.

Keywords: voltage-source converter based multi-terminal direct current (VSC-MTDC); voltage-sourced converter (VSC); power sharing; DC voltage deviation suppression; droop control; model predictive control (MPC)

(编辑 方晶)